

# **Space-Grating Optics in the human retina: a ‘living crystal’ accomplishes human photopic and scotopic vision by means of Fresnel Nearfield Interferences.**

**Norbert Lauinger**

*Institute for Optosensory Systems, Kalsmuntwesthang 9, D – 354578 Wetzlar, Germany  
(norbert@lauinger-web.de).*

## **Abstract.**

The present interpretation of photopic color and scotopic brightness vision is based upon the fact that the pigments of the photoreceptors implement the visible spectrum corresponding to their luminosity curves in RGB-color space and in brightness space. However, if one looks at the cell layers of the retina as phase gratings with differences in the refractive index between the cell nucleus and the cell plasma and if one were to calculate the outer nuclear layer of the retina as a space grating, then the result is that this interference-optically transforms the visible spectrum into RGB-diffraction orders in the Fresnel nearfield behind the space grating. These agree with the wavelengths of the peaks of the cone luminosity curves at 559nmR, 537nmG and 447nmB and by means of an adaptive third grating constant through the merger of R+G at 512nm, they determine the peak of the luminosity curve of the rods.

**OCIS Codes:** (050.0050) Diffraction and gratings; (330.0330) Vision, color, and visual optics; (280.1415) Biological sensing and sensors; (330.1720) Color vision; (330.5370) Physiological optics.

## **Introduction**

The basic question, whether optics or the pigments of the photoreceptors (cones and rods) determine human color and dimlight vision is to be decided with the aid of Fresnel nearfield space grating optics in the visible spectrum (380 - 760nm). The retina of the eye is a layer of brain tissue invaginated into the eye cavity and initially consisting of strung together cells as a planar epithelium. Up until the 7th month before birth there are no photoreceptors in the retina because the differentiation of three cell layers which in histology are termed as nuclear layers takes priority. They consist of cells with a nucleus and cell plasma and they are located between the inner and outer limiting membrane of the retina anterior to the photoreceptors. At a late stage, the photoreceptors grow out of the outer nuclear layer. Since the cell nucleus and the cell plasma are distinguished from one another only due to the differences in the refractive indices, they form optical phase gratings which are completely translucent. It is particularly due to this complete translucency that they have so far been classified as being insignificant for vision and scientists have concentrated exclusively on the photoreceptors and the neuronal nets in the retina. In the middle of the 20th century, the luminosity curves of the pigments in the outer segments of the cones and rods were

measured [Rushton, 1, 1975] and the RGB-curves (Red-Green-Blue) reproduced in Fig.1 with their peaks at 565 - 570nm(R), 535 - 540nm(G), 435 - 445nm(B) for cones and 510 - 515nm for rods were documented.

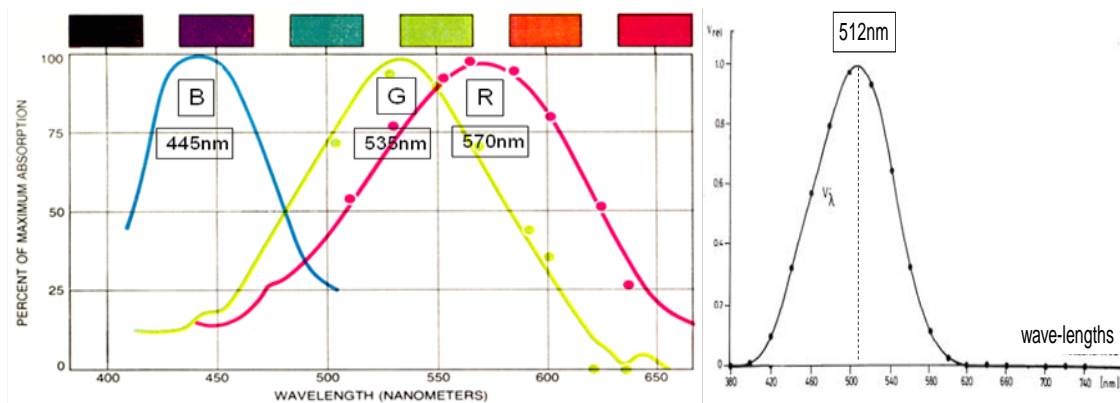


Fig 1: (left) Three luminosity curves of the cones (daylight vision). (right) luminosity curve of the rods (dimlight vision).

With this, the explanation of vision had developed another step further. It became clear that the colors which our eyes see do not exist on the visual objects, but rather exist in the eye only. And it was possible to claim that the pigments in the photoreceptors would accomplish the transformation of the visible light producing the images of the visual objects into the RGB-color space for trichromatic-additive color (daylight) vision and for dimlight vision into the colorless brightness values. It was possible to technically adapt their characteristics for color and black and white films and later for corresponding RGB-CD's. In this way, the world of vision appeared to be sufficiently explained and it seemed to be unnecessary to consider cellular space gratings in brain layers. However, now the explanation of vision can be supplemented with the space grating optical calculations of the author who was the initiator and leader of the NAMIROS-BMBF-project (Nano- und Mikro-Raumgitter für die optische Sensorik [2, 2106-12]). On numerous occasions, Prof. Emil Wolf/Rochester NY, Prof. Adolf Lohmann/Erlangen and Prof. David Casasent/Pittsburgh encouraged him to continue with this work.

**Diffraction space gratings as optical resonators in white X-ray light and in the visible spectrum, interferences in the Fraunhofer farfield and in the Fresnel nearfield behind a space grating.**

Everything new is based upon the past and has its very own charm. A quick review of the history of space gratings optics is to make the following more comprehensible. Crystals are space gratings of solid states composed of atoms. They are diffractive resonators because the wavelengths of the X-ray light are close to the interatomic distances. Due to the fact that as a rule, there are hundreds of atomic layers in a crystalline space grating, monochromatic 'colors' result in their diffractive orders in the white X-ray light. In the case of many organic or inorganic crystals this occurs in transmission or sometimes in reflection. As a rule, transmission is all about measurements in the Fraunhofer farfield behind the space gratings.

Hereafter, we are dealing with calculations and observations in the Fresnel nearfield. Nearfield and farfield are of particular importance in acoustics and in telecommunication engineering and they display different physical characteristics. The nearfield is located directly behind the source of radiation and is marked by interference effects of the waves. The farfield is located at a greater distance behind and displays planar waves in space. The triumph of X-ray crystallography led to the systematic explanation of the structure of elements and molecules right up as far as the explanation of the DNA-structure.

The equations valid for the interferences in the Fraunhofer farfield were formulated at an early stage as the von-Laue and the Bragg equations and they were discussed in some of the classic textbooks on optics. In this way, Bergmann-Schaefer [3, p.296, 1962] described the diffractive effects in the farfield of a three-dimensional grating with cubical packing of point-like atoms and with a multitude of atomic layers as follows: Interference maxima only develop where "light cones centered upon the axes  $x$ ,  $y$ ,  $z$  intersect at the intersection points of hyperbolas and circles and as a rule, that is not the case. Only if the wavelength  $\lambda$  has been selected correctly, this incident can occur in the case of perpendicular incident light. Therefore,  $\lambda$  cannot be selected at random" ... "If you have white light and thus a whole wavelength continuum at your availability, then the space grating will select those wavelength(s) whose three geometric requirements are met. However, in this case, this is not just any ordinal number triple  $h_1h_2h_3$  (whole numbers  $\geq 111$ ) and the diffracted light is no longer white, but monochromatic." This was written based on the understanding of X-ray crystallography. And Bergmann-Schaefer concluded: "Diffraction on a space grating is of no decisive importance in actual optics because no-one had succeeded to create a sufficiently precise space grating for the visible light." This remained unchanged, although Ewald [4, 1965] emphasized the validity of crystal optics also for visible light in his essay titled: "Crystal optics for visible light and x rays". It was only in the laboratory of Prof. A. Lohmann and his students in Erlangen, that Fresnel nearfield optics in its individual aspects (Talbot-, Lau effect, etc.) was researched more closely. Fig 2 (left) shows the positions of the interference maxima in the case of perpendicular incident light in a hexagonal space grating. As opposed to the cubic grating, there are now no two pairs of hyperbolas crossing at  $90^\circ$  with intersection points on the circles, but rather three pairs of hyperbolas crossing at  $60^\circ$ . The interference maxima exist where the light cones centered toward the  $x$ ,  $y$ ,  $z$  axes meet the circles at a particular point.

The geometric conditions for the realization of interferences alone do not lead to concrete resonance wavelengths specifically allowed for interference, developing the so-called chromaticity of the space grating. In the case of only a few grating layers in the space grating, this is also not monochromatic, but rather displays a larger spectral half-height bandwidth as the number of the grating layers is reduced. The space gratings consisting of biological cells with a hexagonal densest packing, with interferences in the Fresnel nearfield, and with non-monochromatic resonance wavelengths therefore display slightly different aspects of diffractive optics than farfield- crystallography optics.

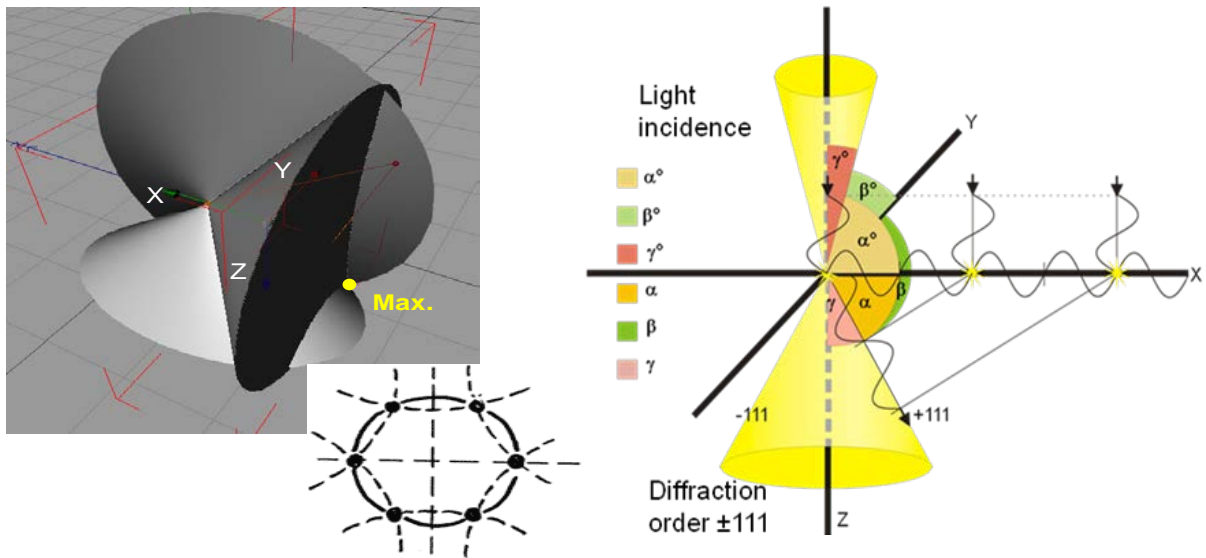


Fig. 2: (left) the interference maxima behind the hexagonal space grating are located in the common intersection points of three light cones representing the intersection points of three pairs of hyperbolas crossing at  $60^\circ$ . (right) The double cone direction cosine connects the light incident ( $\alpha^0$ ,  $\beta^0$ ,  $\gamma^0$ -angle) into the space grating in  $\text{Cos}$ - and/or  $\text{Cos}^2$  segments with the angles of the light ( $\alpha$ ,  $\beta$ ,  $\gamma$  - angle) diffracted into a diffraction order (e.g.  $h_1h_2h_3 = \pm 111$ ).

### The retina as a diffractive space grating in (white) visible light. Geometry and RGB-chromaticity of interferences for color (daylight) vision.

As shown in Fig. 3, the retina disposes of three nuclear layers in which there are cell bodies at graduated sizes: larger ones in the inner (INL-), smaller ones in the middle (MNL-), and smallest cells in the outer (ONL-) nuclear layer [Bargmann, 5, 1967]. Blechschmidt [6, 1967] documented the successive differentiation of the three layers which takes seven months within the pre-natal period of time. The cells of the ONL-layer are the ones representing the space grating which is hereafter deemed to be responsible for color and dimlight vision. The distances between the cells - the so-called grating constants - in the case of the hexagonal densest packing are close to the visible wavelengths. Just before birth photoreceptors (cones and rods) grow out of this layer through the outer limiting membrane of the retina into the space behind the retina. The number of the cell layers in the ONL-space grating amounts to approximately 3-6 layers. They exist throughout from the center (fovea) as far as the far periphery of the retina. Due to the fact that the nuclear layers are located lightwards before the photoreceptors, the retina is named 'inverted retina'.

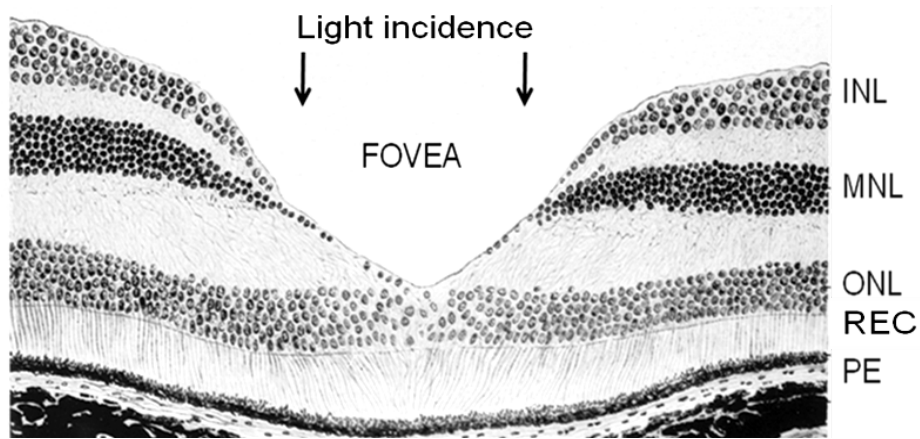


Fig.3: The three nuclear layers of the 'inverted' retina of the eye are located lightwards before the layer of photoreceptors (REC). In the fovea, the location of the most acute vision in daylight vision, there are exclusively cones (PE = pigment epithelium).

The calculation of the geometrical requirements which the diffraction orders have to meet in order to allow resonance wavelengths for daylight (color) vision, represents the first step of the calculations. The space grating optical basis of dimlight vision is then examined as a second step. As in the review of X-ray crystallography, the calculation starts with the double cone direction cosine reduced to a beam of light perpendicularly incident into the space grating (Fig.2 right). As in the von-Laue-equation, the  $\text{Cos } \alpha, \beta, \gamma$  - segments in the direction cosine describe three light cones centered towards the axes  $x, y, z$  which have to intersect at common points in the space, namely at the locations of the constructive interferences. The  $\alpha^\circ, \beta^\circ, \gamma^\circ$ -angles represent the angles in the light cone of the light incident into the space grating. The double cone direction cosine reads as follows:

$$\left(\text{Cos } \alpha - \text{Cos } \alpha^0\right)^2 + \left(\text{Cos } \beta - \text{Cos } \beta^0\right)^2 + \left(\text{Cos } \gamma - \text{Cos } \gamma^0\right)^2 = 1$$

In the equations (1a) and (1b) which are identical, but describe different aspects, the light cones incident into the space grating are reduced to a perpendicular light beam. In this  $\alpha^\circ$  and  $\beta^\circ = 90^\circ$ , and thus their  $\text{Cos} = 0$ , and  $\gamma^\circ = 0^\circ$  with the  $\text{Cos } \gamma^0 = 1$ .

$$\left(\text{Cos}^2 \alpha + \text{Cos}^2 \beta + \text{Cos}^2 \gamma\right) - 2 \text{Cos } \gamma \text{Cos } \gamma^0 = 0 \quad (1a)$$

$$\frac{2 \text{Cos } \gamma \text{Cos } \gamma^0}{\text{Cos}^2 \alpha + \text{Cos}^2 \beta + \text{Cos}^2 \gamma} = 1 \quad (1b)$$

Specific data are achieved if one includes the hexagonal geometry of the grating constants  $g_x, g_y, g_z = 2 : \sqrt{3} : 1$  as shown in Fig.4 (left) into the equation; moreover the  $\text{Cos } \alpha, \beta, \gamma$  - segments of the von-Laue-formulation ( $\text{Cos } \alpha = h_1 \lambda / g_x$  etc.) for the farfield must be rewritten into the Fresnel form of the nearfield ( $\text{Cos } \alpha = h_1 g_x / s$ ). In which way the dimension  $s$  is connected to  $\lambda$  will become clear in a moment. Last but not least, the  $h_1 h_2 h_3 = 111$  - triple

must also be included. It designates the fundamental wave  $\lambda_{111}$ , upon which the space grating is to be tuned. This is completely analogous to the way in which the resonance body of any instrument needs to be tuned in order to create harmonic waves ( $\lambda_{h_1h_2h_3}$ ).

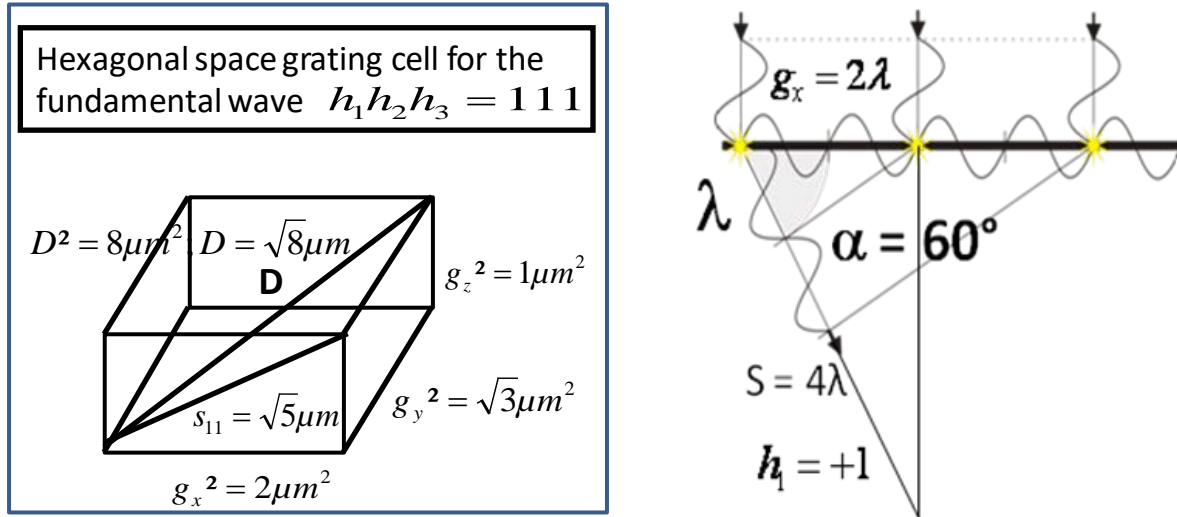


Fig.4: (left) Spatial Pythagoras in the hexagonal space grating for the 111-fundamental wave; (right) reformulation of the Cos-segments of the von-Laue version  $\text{Cos}\alpha = h_1\lambda/g_x = \lambda/2\lambda = 0.5$  into the Fresnel version  $\text{Cos}\alpha = h_1g_x/s = 2\lambda/4\lambda = 0.5$ , by means of which in each case the angle  $\alpha = 60^\circ$  results.

The crystal-optical resonance factor [Ewald, 4, 1965] allows for the calculation of the dimension  $s$  for the fundamental wave  $\lambda_{111}$  in equation (2) and (3). It appears that  $s_{111}$  corresponds to the right term in equation (2) and has the dimension  $4\mu m$ . The dimension of  $\nu\lambda$  is  $\mu m \times \mu m^{-1}$ .

$$\nu\lambda = \frac{2h_3g_z}{h_1^2g_x^2 + h_2^2g_y^2 + h_3^2g_z^2} \times \frac{h_1^2g_x^2 + h_2^2g_y^2 + h_3^2g_z^2}{2h_3g_z} = 1 \quad (2)$$

$$s_{111} = \frac{h_1^2g_x^2 + h_2^2g_y^2 + h_3^2g_z^2}{2h_3g_z} = \frac{4+3+1}{2} = \frac{8}{2} = 4 \quad (3)$$

Thanks to these few, but decisive approaches, the geometric requirements upon the optics of the hexagonal space grating have been explained. These must be met by the specific resonance wavelengths. Fig.5 illustrates (left) the crystal-optical resonance factor  $\nu\lambda$ , a constant in the product of wavelength and frequency and (right) the periodicity of typical Fresnel nearfield interferences behind a diffractive line grating which is named a Talbot-/Lau-carpet. For further information please refer to Lauinger [7] and Tomandl [9]. In the case of the space gratings, interferences develop corresponding to a three-dimensional light tissue in the Fresnel nearfield space.

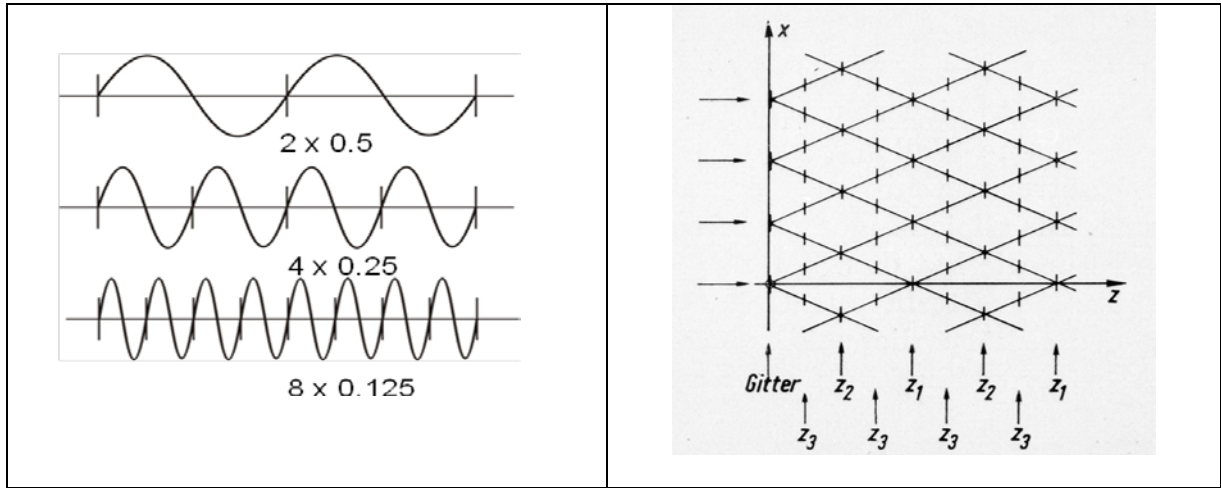


Fig. 5: (left) crystal-optical resonance factor  $v\lambda$ , (right) typical Fresnel-Talbot-Lau-Interferences in Talbot planes behind a simple line grating [Menzel-Mirandé-Weingärtner, 8, 1973 and Tomandl, 9, 2010].

The equations (1a) and (1b) with the data so far lead to the results in (4a) and (4b) for the fundamental diffraction order  $h_1h_2h_3 = 111$  resp. the fundamental wave  $\lambda_{111}$ .

$$\left(\frac{h_1g_x}{s_{111}}\right)^2 + \left(\frac{h_2g_y}{s_{111}}\right)^2 + \left(\frac{h_3g_z}{s_{111}}\right)^2 - \frac{2h_3g_z}{s_{111}} = (0.25 + 0.1875 + 0.0625) - 0.5 = 0.5 - 0.5 = 0 \quad (4a)$$

$$v_{111}\lambda_{111} = \frac{2h_3g_zs_{111}}{h_1^2g_x^2 + h_2^2g_y^2 + h_3^2g_z^2} = \frac{2 \times 4}{4 + 3 + 1} = \frac{2}{8} \times \frac{8}{2} = 0.25 \times 4 = 1 \quad (4b)$$

Each of the two equations covers one of two aspects of the diffractive incident: equation (1a and 4a) describe the spatial Pythagoras (in the well-known simple formulation of  $a^2 + b^2 + c^2 - d^2 = 0$ ) in the hexagonal space grating cell in Fig. 4 (left) and equation (1b and 4b) describe the crystal-optical resonance factor  $v\lambda$  (in the simplest formulation:  $v\lambda = d^2/(a^2+b^2+c^2) = 1$ ). Both geometric requirements prove to be related in some aspects to the von-Laue farfield equation, but are fundamentally different due to the reciprocal Fresnel formulation of the Cos-segments and the particularity of the hexagonal densest packing of the cells making up the space grating.

In order to be able to arrive at a statement regarding the resonance wavelengths and thus about the chromatics of the space grating, further considerations are necessary. Since as opposed to e.g. the cubic grating in the hexagonal space grating, the grating constant  $g_y$  is strictly connected to  $g_x$ , only the grating constants  $g_x$  and  $g_z$  represent free resonance enabled dimensions. Together they make up the angled sender antenna of a resonator. Its product for the fundamental wave  $\lambda_{111}$  is the diagonal  $s_{11} = \sqrt{g_x^2 + g_z^2} = \sqrt{5}$ . If one tunes or

transforms  $s_{111}$  to  $\lambda_{111}$  in equation (5), with  $s_{111}\lambda_{111} = 4\lambda_{111} = s_{11} = \sqrt{5}$  the resonance fundamental wave  $\lambda_{111} = 559\text{nm}$  results.

$$\lambda_{111} = \frac{2h_3g_zs_{111}\lambda_{111}}{h_1^2g_x^2 + h_2^2g_y^2 + h_3^2g_z^2} = \frac{2 \times 1 \times 1 \times 4\lambda_{111}}{4 + 3 + 1} = \frac{2s_{11}}{8} = \frac{s_{11}}{s_{111}} = \frac{\sqrt{5}}{4} = 0.559\mu\text{m} \quad (5)$$

If one then examines all of the 24 low diffraction orders by varying the  $h_1h_2h_3$ -triples from 111 to 333, then in addition to the fundamental wave 559nm(R) only two harmonic waves with  $\lambda_{123} = 537\text{nm}$ (G) und  $\lambda_{122} = 447\text{nm}$ (B) result.

$$R = \lambda_{111} = \frac{2 \times 1 \times 1 \times \sqrt{5}}{4 + 3 + 1} = \frac{2\sqrt{5}}{8} = \frac{\sqrt{5}}{4} = 0.25\sqrt{5} = 0.559\mu\text{m}$$

$$G = \lambda_{123} = \frac{2 \times 3 \times 1 \times \sqrt{5}}{4 + 12 + 9} = \frac{6\sqrt{5}}{25} = \frac{\sqrt{5}}{4.166} = 0.24\sqrt{5} = 0.537\mu\text{m}$$

$$B = \lambda_{122} = \frac{2 \times 2 \times 1 \times \sqrt{5}}{4 + 12 + 4} = \frac{4\sqrt{5}}{20} = \frac{\sqrt{5}}{5} = 0.20\sqrt{5} = 0.447\mu\text{m}$$

Since these three wavelengths correspond to the peak values of the luminosity curves of the cones in Fig.1 (left), they form the sought after RGB-triple of the resonance wavelengths of the retinal space grating and describe their RGB -chromaticity in color vision. In this way, the fundamental question has been answered that space grating optics in the Fresnel nearfield - and not the photo pigments - in color (daylight) vision has the ability to perform the transformation of the visible spectrum into the RGB color space. (Aside from the RGB-triples, a low-intensity resonance represents only a triple 213 with  $\lambda_{213} = 479\text{nm}$ . It possibly causes the thus far unexplained kink in the R-curve in Fig. 1).

Fig. 6 (left) illustrates the RGB-sequence of the three diffraction orders with six interference maxima in color vision in each case. Since the R-maxima are located innermost and the G-maxima outermost on a circle, there is no overlapping between R and G as in the luminosity curves of the cones in Fig.1. Fig.6 (right) illustrates the complete RGB-Fresnel nearfield transmission system with the space grating being the resonator (angled sender antenna with  $g_x$  and  $g_z$  as the 'tuning fork' with  $s_{11} = \sqrt{(g_x^2 + g_z^2)}$  as the resonance diagonal), with the standing RGB-spherical waves, and the RGB-outer segments of the photoreceptors (cones) being the receiver antennae. The resonance diagonal  $s_{11} = \sqrt{5}$  represents  $4\lambda_{111}\text{R}$ ,  $4.167\lambda_{123}\text{G}$  and  $5\lambda_{122}\text{B}$  with two integers as standing waves. A 6x magnification of the hexagonal cell leads to  $s_{11} = \sqrt{(12^2 + 6^2)} = \sqrt{180} = 13,42\mu\text{m}$ . All three resonance wavelengths are than integers with  $24\lambda_{111}\text{R}$ ,  $25\lambda_{123}\text{G}$  and  $30\lambda_{122}\text{B}$ . With the  $13,42\mu\text{m}$  length they eventually could bridge over the distance between the ONL-layer or the outer limiting membrane of the retina and the outer segments of the cones. Such transmission systems are widely used in telecommunications. Fresnel nearfield optics corresponds to nearfield computing which is increasingly used today.

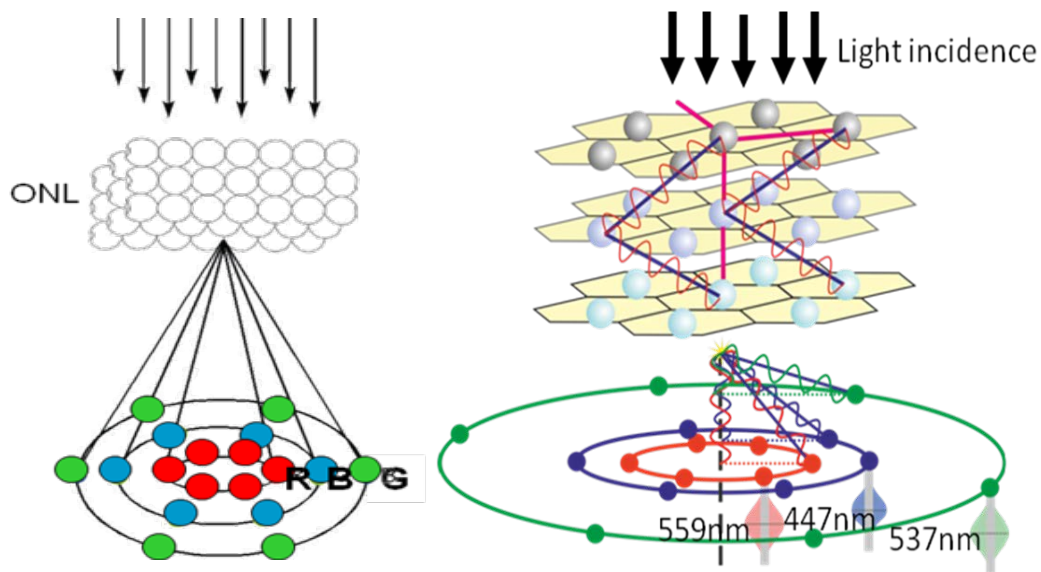


Fig. 6: Sequence of the RGB-diffraction orders with R in the smallest (innermost) circle, B in the larger (middle) circle and G in the largest (outermost) circle with six interference maxima in each case. (right) complete RGB-Fresnel transmission system with the space grating as the sender, the standing RGB-spherical waves, and nano-antennae of the outer segments of the cones.

**The calculation of dimlight vision and/or the Purkinje-Shift from color (daylight) vision to dimlight and vice versa.**

Only if dimlight vision as well as daylight vision can be explained, a new interpretation of the retinal fundamentals in vision will succeed. Purkinje has described the observation of how during the transition from daylight to dimlight vision, a blue flower will appear brighter and a red rose darker. This shift was more easily explained after the luminosity curve of the rod pigments shown in Fig.1 (right) had been measured spectrophotometrically. Now it became possible to attribute the responsibility for the shift of the peak of luminosity to approx. 510 - 520nm to the pigments of the rod receptors. Thus, it was possible to conclude that the Purkinje-Shift had been photo-chemically explained. In RGB space grating optics it is now identified to be an adaptive optical shift. Fig.7 (left) shows that in the case of a low adaptive reduction of  $g_z$  from  $1\mu\text{m}$  to  $0.912\mu\text{m}$ , a merger of the RG-diffraction orders takes place at the spectral location of 512nm and at the same time the B-diffraction order becomes nearly insignificant. The RGB-trichromaticity becomes an RG(B)-achromatism. Fig.7 (right) illustrates the corresponding relative position of the RG(B)-diffraction orders. Thus, R and G are both similarly colorless. In a rather hidden annotation in his book on color metrics, Erwin Schrödinger expressed the suspicion that only R and G together could be able to determine dimlight vision [Lauinger, 7, 2014].

Based on equation (5) the space grating optical RG(B) triple for dimlight vision results with the diagonal  $s_{11} = \sqrt{(2^2 + 0.912^2)} = \sqrt{4.83}$  of the fundamental wavelength  $\lambda_{111}$ :

$$R: \lambda_{111} = \frac{2h_3g_z\sqrt{(h_1^2g_x^2 + h_3^2g_z^2)}}{h_1^2g_x^2 + h_2^2g_y^2 + h_3^2g_z^2} = \frac{2 \times 1 \times 0.912 \times \sqrt{4.83}}{4 + 3 + 0.912^2} = \frac{4.01}{7.83} = 0.512\mu m$$

$$G: \lambda_{123} = \frac{2 \times 3 \times 0.912 \times \sqrt{4.83}}{4 + 12 + 7.486} = \frac{12,026}{23,486} = 0.512\mu m$$

$$B: \lambda_{122} = \frac{2 \times 2 \times 0.912 \times \sqrt{4.83}}{4 + 12 + 3.327} = \frac{8.017}{19.327} = 0.415\mu m$$

All three RG(B) wavelengths with their specific  $s_{11}h_2h_3$  values in equation (3) ( $s_{111} = 4.294$ ,  $s_{123} = 4.292$ ;  $s_{122} = 5.298$ ) fulfill the geometric resonance conditions of the spatial Pythagoras in equation (4a) and of the  $v\lambda$ -factor in (4b). However, a resonance comparable to the RGB-triple of color vision is not achieved, i.e. the wavelengths 512nm (R and G) and 415nmB do not form whole-number standing waves on an  $s_{11} = \sqrt{(g_x^2 + g_z^2)}$ -sender antenna. This particularity remains reserved to the qualitatively more complex color vision. If one were to imagine that in the course of evolution, color vision had developed on the basis of dimlight vision, then an extension of the grating constant  $g_z$  of the ONL-grating by  $0.088\mu m$  would have been sufficient to achieve the RGB-resonance situation suitable for color vision.

With these space grating optical calculations, it has been explained also for dimlight vision that Fresnel nearfield space grating optics is able to undertake the associated transformation of visible light into the RG(B)- space of scotopic brightness vision.

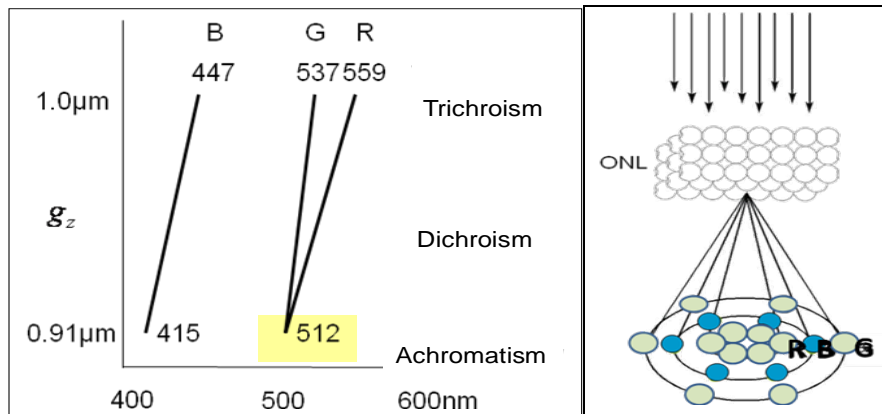


Fig. 7: (left) space grating optical explanation of the Purkinje-Shift, (right) arrangement of the RGB(B) diffraction orders in Fresnel space behind the ONL-space grating.

### Does a chromatic adaptation of color vision become possible with $g_z > 1\mu m$ above the RGB-triple 559/537/447nm?

When looking at the spectro-photometrical or now also at the space grating optical RGB-data related to color vision, the objection is often raised that with the fundamental wave  $R = 559\text{nm}$  in the RGB-triple, it is impossible to create a true perception of red colors. However, the space grating optical calculation is able to show by means of the theoretical extension of

the grating constant  $g_z$  from  $1\mu\text{m}$  to  $>1\mu\text{m}$  that the R-fundamental wave with its GB-harmonics could adaptively shift to longer wavelengths. The example with  $g_z = 1.1\mu\text{m}$  and  $s_{11} = \sqrt{5.21}$  in Fig.8 via equation (5) leads to the RGB-triple  $612\text{nmR}$ ,  $560\text{nmG}$ , and  $482\text{nmB}$ ; an RGB-triple of  $630\text{nmR}$ ,  $568\text{nmG}$  and  $494\text{nmB}$  results with  $g_z = 1.135\mu\text{m}$  and  $s_{11} = 2.3\mu\text{m}$ . In the very same way, any other RGB-triple with  $g_z > 1\mu\text{m}$  can be demonstrated.

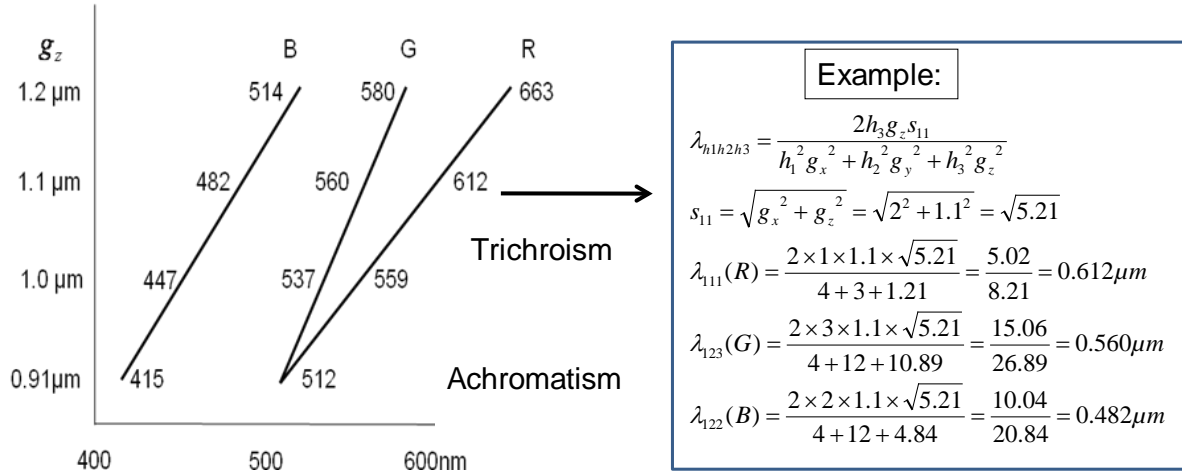


Fig.8: (left) Could the 3rd grating constant  $g_z$  in the space grating allow an adaptive transition from achromatism to trichromacy which can be extended by  $g_z > 1$ ? (right) exemplary calculation for an RGB-triple with  $612\text{nm(R)}$ ,  $560\text{nm(G)}$ , and  $482\text{nm(B)}$ .

Theoretically the third grating constant  $g_z$  could then possibly assume the role of the chromatic RGB-adaptation to different spectral constellations and would thus adaptively design the complete range from achromaticity in dimlight vision (Purkinje-Shift) via the dichromaticity to a variable trichromacy of color vision. Upon closer inspection of the data, however, it becomes apparent that such a theoretically possible adaptivity does not occur. The calculations with  $g_z > 1$  show that all the RGB triples with  $g_z > 1\mu\text{m}$  fulfill the spatial Pythagoras and the  $v\lambda$ -resonance factor condition, but the  $s_{11}$ -diagonal values of the sender antenna no longer result in a whole number  $\lambda_{111}(R)$ -periodicity. (In the exemplarily selected RGB-triple with  $612\text{nmR}$ ,  $s_{11} = 3.7 \lambda_{612}$ , in the RGB-triple with  $630\text{nmR}$   $s_{11}$  results in  $3.65 \lambda_{630}$ ). The result is the same as for the RG(B)-triple of dimlight vision. Therefore it seems to be obvious to conclude that human color vision is based exclusively on the RGB  $559/537/447\text{nm}$ -resonance solution. This interpretation of the data revises the opinion on this topic as presented in [12]. The adaptation to different spectral constellations occurs in a different way to the one supposed here theoretically. Since the RGB-diffraction orders in a space grating with only a few layers exhibit a large width at half-height, the long-wave parts of the visible spectrum find sufficient entry into the RGB- color channel in order to support fully valid red perceptions.

**The retinal space grating as a ‘living crystal’: the coupling and decoupling of the three grating constants and the aperture angles of the light cones of the diffracted light.**

So far, no indications regarding the aperture angles of the light cones in the RGB- diffraction orders have been made. In connection with the question regarding the coupling and decoupling of the three grating constants, this will now be caught up on. The calculation of

the  $\alpha$ ,  $\beta$  and  $\gamma$  angles is carried out via the parts of equation (6) into whose denominator the sought for value  $s_{h_1h_2h_3}$  from equation (3) is integrated. In Fig.9 only the  $\gamma$ - aperture angles directed towards the z-axis are shown.

$$\cos\alpha = \sqrt{\left(\frac{h_1g_x}{s_{h_1h_2h_3}}\right)^2}; \cos\beta = \sqrt{\left(\frac{h_2g_y}{s_{h_1h_2h_3}}\right)^2}; \cos\gamma = \sqrt{\left(\frac{h_3g_z}{s_{h_1h_2h_3}} - 1\right)^2} \quad (6)$$

The upper line of Fig.9 shows the  $\gamma$  - angles for the RGB-chromaticity in color vision for the hexagonal space grating cell with  $g_x : g_y : g_z = 2 : \sqrt{3} : 1\mu\text{m}$ :  $41.4^\circ$  for 559nmR,  $74.0^\circ$  for 537nmG and  $53.0^\circ$  for 447nmB. The bottom line on the left half of the figure shows the  $\gamma$  - angles for the RG(B)-chromaticity in dimlight vision for the same space grating cell:  $38.0^\circ$  for 512nmR,  $69.0^\circ$  for 512nmG and  $49.0^\circ$  for 415nmB. The reduction of  $g_z = 1\mu\text{m}$  to  $g_z = 0.912\mu\text{m}$  in the Purkinje-Shift causes a small diminution of the  $\gamma$ -angles. All angles show the RBG-sequence of the light cones as illustrated in Fig.6.

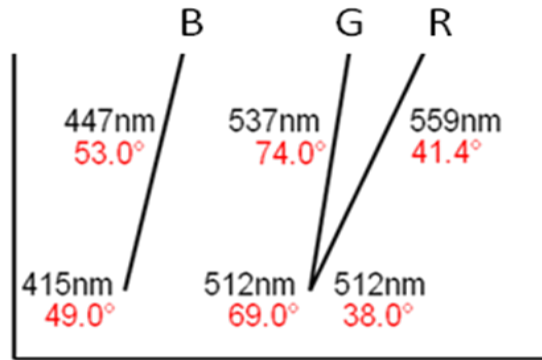


Fig.9:  $\gamma$ -angles of the diffraction order light cones and RGB-chromaticity for the RGB-triples with R = 559nm and R = 512nm in the Purkinje-Shift.

At the transition from color vision to dimlight vision the space grating cell changes from a thicker hexagonal box to become a thinner box. The grating constant  $g_z$  controls the adaptive transition of the RGB-chromaticity in color vision to the RG(B) achromatism in dimlight vision. In this way, the cellular space grating behaves like a 'living crystal' [Geguzin, 10, 1985]. The decoupling of the grating constant  $g_z$  from  $g_x$  and  $g_y$  leads to a modification of the micro-geometry of the cells and introduces the ability to achieve adaptive functionalities. Similar functionally adaptive cell geometry deformations from spheres into rotational ellipsoids were also found during research on acoustics in the human inner ear. In the case of a percentagewise equal enlargement of the three grating constants, i.e. in the case of maintaining a strong coupling of the three grating constants, the  $\gamma$ -angles and RGB-chromaticities of both lines remain constant; the space grating behaves like an inflatable hexagonal box. In the case of a whole number multiplication of  $g_x$  and  $g_z$ , the resonance diagonal  $s_{11} = \sqrt{(g_x^2 + g_z^2)}$  becomes a whole number multiple of  $\lambda_{111}(R)$  and  $\lambda_{122}(B)$ , thus corresponding to the resonance requirement. At  $V = 6x$ , with  $s_{11} = \sqrt{180}$  all three resonance wavelengths become whole numbers for the first time ( $24\lambda_{111}$ ;  $25\lambda_{123}$ ,  $30\lambda_{122}$ ). The length of  $s_{11}$  then amounts to  $13.42\mu\text{m}$  and may correspond to the distance between the outer limiting membrane of the retina and/or the ONL-space grating and the outer segments of the cones.

## Advantages of Fresnel nearfield space grating optics.

As opposed to the Fraunhofer farfield, the available information about the visual objects in the optical image is fully retained in the Fresnel nearfield and is not transformed into a power spectrum. The processing of the image in the three retinal grating layers corresponds to layered processing of information proven to occur in the visual cortical centers (CGL and V1). Three cell gratings, which are graduated in their grating constants and overlap one another form 'optical pillars' as shown in Fig. 10. In these, the RGB-chromaticity exists in circular fields which can become the basis for overlapping, neuronal 'receptive fields'. The top-down view upon planes behind two graduated and superimposed gratings (right: top with  $g_x = 100\mu\text{m}$  and  $20\mu\text{m}$ ; center with  $g_x = 16\mu\text{m}$  and  $8\mu\text{m}$ ) shows these diffractive optical, digitally gridded fields. In this process, (bottom right) the image of an object in a Talbot plane behind the 2nd grating is completely retained. The microscopic photographs (right) were created as part of the NAMIROS-BMBF project [2] at the Fraunhofer-Institut IAP/Golm.

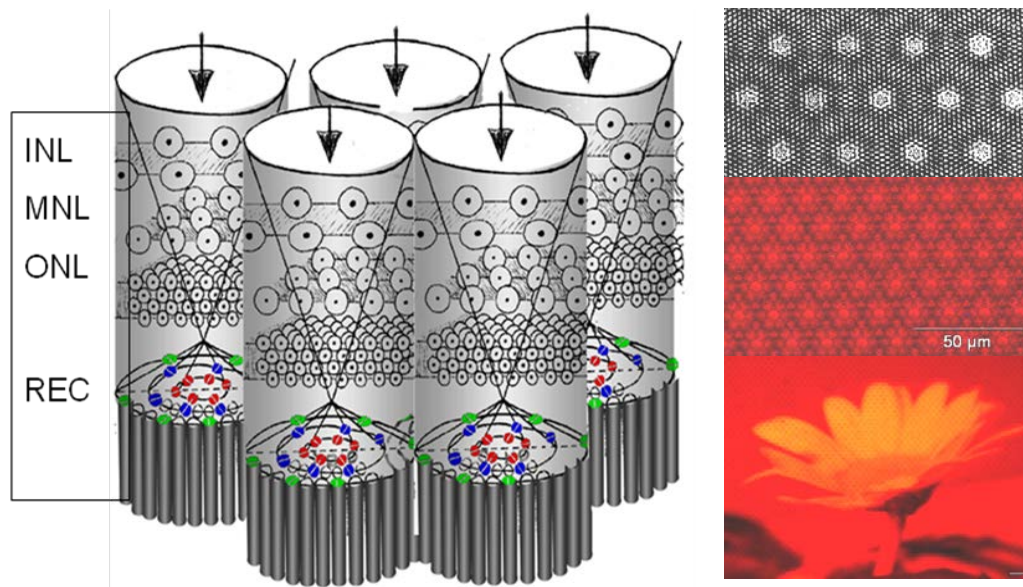


Fig. 10: (left) three cell gratings graduated in their grating constants and superimposed upon one another form 'optical columns', circular fields, and pixelated object images.

Since the diffraction of the visible occurs in the RGB-space, i.e. in the so-called 'reciprocal grating space' of crystal physics, a new interpretation of the 'inversion' of the retina arises as a result. Some aspects, in particular the temporal bringing forward of the development of the nuclear layers in the prenatal period to before that of the photoreceptors indicates that they take on the significance of a 'pacemaker' to higher cognitive and thus 'cortical' functions in the eye in the evolution of human vision. The fact that interference optics plays a decisive role in this becomes plausible by means of the simple observation that upon closing one eye in binocular vision the luminosity is not halved. In wave optics, any deviation from the principle of the additivity of luminosities is an indication towards interference.

## Summary and outlook

The calculations of the Fresnel nearfield space grating optics prove for human vision that the decisive transformations of the visible spectrum into the RGB-space of color vision (peaks of

the luminosity curves at 559nmR, 537nmG and 447nmB) and into the RG(B)- space of dimlight vision (peaks at 512nmR, 512nmG and 415nmB) are realized by means of optics and not by means of the pigments of the photoreceptors. In this way, the photo pigments would be programmed by optics. The adaptive retinal space grating becomes comparable to a 'living crystal'. With the explanation of the space grating optical functionalities in color and in dimlight vision, also a brain layer in the eye became understood much better. The 'inverted' retina shifts the basis of vision into the 'reciprocal grating space' of crystal optics, but due to the Fresnel nearfield processing maintains full information about the imaged objects. The task remains to confirm the calculated data experimentally. Another effect - the optical relativization of the seeing of local colors to the global illumination in object space - was discussed in [12] and in [11] aside from a discussion of the data presented here. The practical relevance of the data is considered in connection with the development of future retina implants on the basis of Fresnel nearfield space grating optics.

## Bibliography

1. W.A.H. Rushton, "Visual Pigments and Color Blindness, *Scientific American*, **232** (3), 1975.
2. NAMIROS-BMBF-Projekt 13N9040 „Nano- und Mikro-Raumgitter für die Optische Sensorik“, 2006-2012.
3. Bergmann-Schaefer, *Lehrbuch der Experimental-Physik Bd.III,1. Wellenoptik*, (Walter de Gruyter 3/1962).
4. P.P. Ewald, "Crystal optics for visible light and x-rays". *Reviews of Modern Physics*, 37(1), 46-56 (1965).
5. W. Bargmann, *Histologie und mikroskopische Anatomie des Menschen*. (Thieme-Verlag, Stuttgart, 1967).
6. E. Blechschmidt, „Die Entwicklungsbewegungen der menschlichen Retina zur Zeit der Irisentstehung“, *Ophthalmologica*, **154**, 531-550, 1967.
7. N. Lauinger, N., *The Human Eye: an Intelligent Optical Sensor (The Inverted Human Retina: a Diffractive-optical Correlator)*, (IFSA Publishing, 2014) (Open Source in 2017).
8. C. Menzel, M. Mirandé, and I. Weingärtner, *Fourier-Optik und Holographie*, (Springer Verlag, 1973).
9. M. Tomandl, *Realisierung von optischen Talbot- und Talbot-Lau-Teppichen*, Diploma Univ. Wien/Physik (2010).
10. Ja. E. Geguzin, *Lebender Kristall* (Verlag Harri Deutsch, Thun/Frankfurt, 1985).
11. N. Lauinger, "Space grating optical structure of the retina and RGB-color vision". *Applied Optics*, Vol.56, No.4, February 1 2017, pp. 1261 – 1265.
12. N. Lauinger, "Fresnel Nearfield Space-Grating Optics in the human retina explains human color and dimlight vision". IFSA-Publishing in 'Advances in Optics', (posted 23 August 2017, in press) (open source).